High-Throughput, Lysis-free Screening for Sulfatase Activity Using *Escherichia coli* Autodisplay in Microdroplets

Bert van Loo[a,1,*], Magdalena Heberlein[a,b,1], Philip Mair[b], Anastasia Zinchenko[b], Jan Schüürmann[c], Bernard D. G. Eenink[a], Carina Dilkaute[c], Joachim Jose[c], Florian Hollfelder[b], and Erich Bornberg-Bauer[a]

[a]Institute for Evolution and Biodiversity, University of Münster, Germany
[b]Department of Biochemistry, University of Cambridge, United Kingdom
[c]Institute of Pharmaceutical and Medicinal Chemistry, University of Münster, Germany
[1]Both authors contributed equally
[*]corresponding author: b.vanloo@uni-muenster.de

November 26, 2018

Abstract

Directed evolution of enzymes toward improved catalytic performance has become a powerful tool in protein engineering. To be effective, a directed evolution campaign requires the use of high-throughput screening. In this study we describe the development of a high-throughput lysis-free procedure to screen for improved sulfatase activity. For this purpose we combine the use of microdroplet-based single-variant activity sorting with *E. coli* autodisplay. This setup allows circumventing complications arising from cell lysis during screening for enzymatic activity. We successfully displayed the moderately efficient (k_{cat}/K_M = 4.8×10^3 s^{-1} M^{-1}) homodimeric arylsulfatase from *Silicibacter pomeroyi* (*Sp*AS1) on the surface of *E. coli*. For the first step in a 4-step screening procedure we quantitatively screened >10^5 *Sp*AS1 variants for improved sulfatase activity using fluorescence activated droplet sorting. The display of the sulfatase variants on living *E. coli* cells ensured the continuous linkage of genotype and phenotype during droplet sorting. It allowed for direct recovery by simple regrowth of the sorted cells, enriching the percentage of improved variants. When compared to a system involving cell lysis prior to activity measurements during screening, the use of autodisplay on living cells simplified and reduced the degree of liquid handling during all steps in the screening procedure to the single event of simply mixing substrate and cells. The screening procedure allowed us to identify 16 *Sp*AS1-variants with 1.1- to 6.2-fold improved catalytic efficiency compared to wild type, toward the model sulfatase substrate 4-nitrophenyl sulfate. All beneficial mutations occurred in positions that were difficult to predict, i.e. no conserved active site residues were directly affected. The combination of five such mutations as observed in the best variants finally resulted in an *Sp*AS1 mutant with 28-fold improved catalytic efficiency (k_{cat}/K_M = 1.35×10^5 s^{-1} M^{-1}) compared to the wild type.

Keywords

directed evolution; *E. coli* surface display; microdroplets; high-throughput screening; arylsulfatase

Introduction

Directed evolution comprises repeated cycles of mutation,[1–4] followed by selection of variants with improved desired function.[5,6] Directed evolution has been used successfully to improve several enzyme properties such as enantioselectivity,[7–9] operational stability,[10–12] and catalytic efficiency.[13,14] Effective enzyme engineering by directed evolution requires fast, sensitive and reliable screening of large libraries of enzyme variants in order to select the very few improved variants present in these libraries. Current methods for large-scale library testing such as colorimetric colony screening[8,15] or growth selection-based systems[16,17] suffer from narrow dynamic ranges, i.e. they are either too sensitive (almost all variants appear equally active) or too selective (almost all variants appear inactive), limiting the degree of improvement that can be reached. Microtiterplate-based screening methods have a broader dynamic range,[18] but require extensive instrumentation and consumables.

Over the last decade, water-in-oil emulsion microdroplets have been established as a cost and resource effective alternative for efficient high-throughput screening. Microdroplets are *in vitro* compartments and are, in essence, miniaturized reaction vessels that can be created at high frequency (>8 kHz) and in high numbers ($\sim 10^7$ per day).[19–22] Each droplet contains, as a result of a controllable Poisson distribution, on average less than one library variant (in this study $\lambda = 0.35$). In such a library the corresponding protein is produced *in vitro* from a single plasmid copy,[23,24] or by single cells, typically bacteria[21,25] or yeast,[19] each harboring one library variant. Reaction progress in microdroplets can be monitored at high frequencies (>2 kHz), using either commercial fluorescence-activated cell sorters[22] (for sorting water-in-oil-in-water double emulsion droplets), or custom-made on-chip sorters.[19,21,25] For the latter a range of optical signals reporting on reaction progress is now available,[26] based on fluorescence,[27] absorbance,[28] or anisotropy.[29]

In many cases, directed evolution campaigns that screened for single variants required an intrinsic physical link between genotype and phenotype,[30] e.g. using phage display for antibody evolution. Such display methods can also be adapted to screen for single turnover reactions,[31–34] but screening for multiple turnover catalysis, the hallmark of efficient enzymes, is not possible with these methods. In droplet-based screening procedures, the phenotype can be the result of e.g. a fluorescent reaction product formed by multiple turnovers of substrate. During droplet sorting this phenotype stays linked to its genotype (the variant DNA) due to the boundary of the micro-droplet. For both display and many of the droplet-based methods, the genotypes need assistance in order to be recovered after droplet sorting: e.g. for phage display transfection of fresh *E. coli* is required and for lysis-based screening with single *E. coli* cells the plasmid DNA needs to be re-transformed.

In our study we combine a self-replicating genotype, i.e. a living *E. coli* cell, that autodisplays our enzyme of interest on its surface, with activity-based droplet sorting to select for improved performance of multiple turnover reactions. This combination has thus far only been reported for yeast.[19] Autodisplay uses the β-barrel and the linker domain of a natural type V autotransporter protein for displaying the passenger, i.e. the enzyme, to the cell surface (Figure S1).[35,36] Anchoring of the enzyme within the outer membrane by the β-barrel results in its mobility on the cell surface. Thus, we present a system in an easy-to-use lab organism

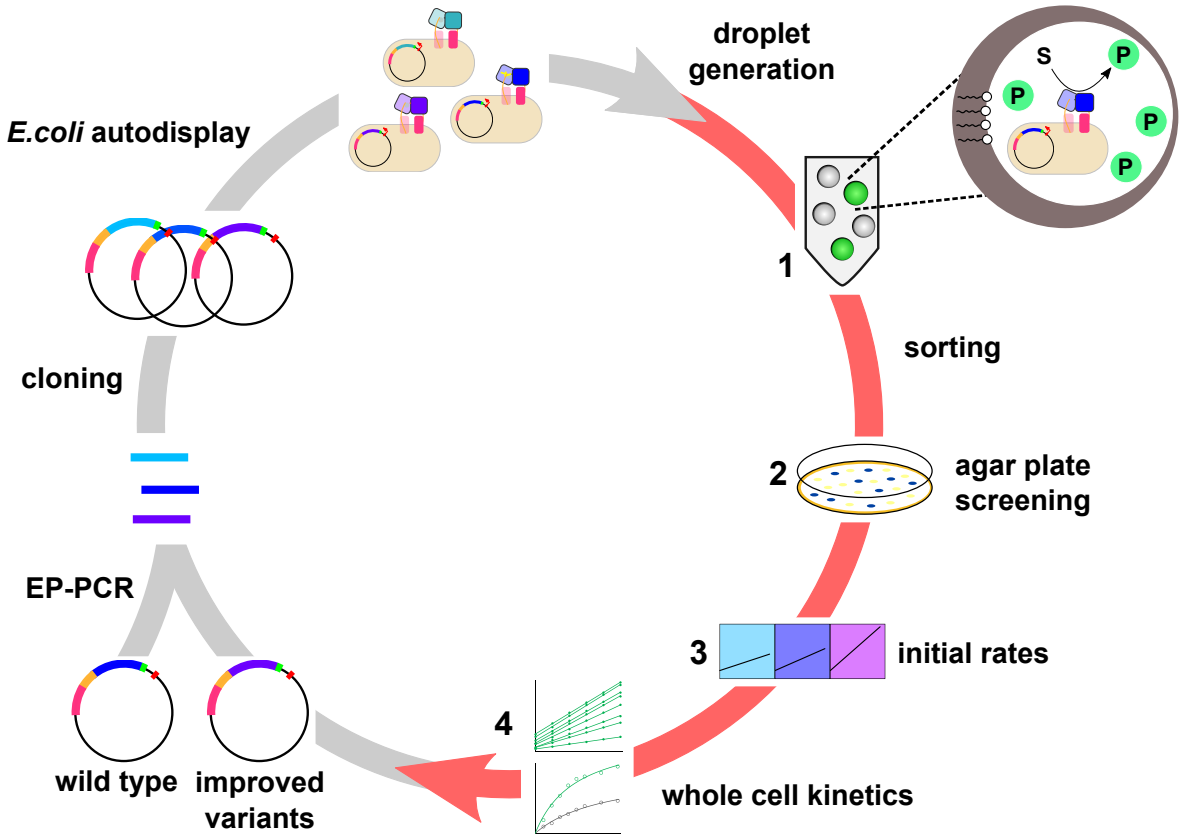

Figure 1: Directed evolution workflow for screening for improved catalytic activity of an autodisplayed dimeric arylsulfatase. A library of arylsulfatase mutants, generated by error-prone PCR (EP-PCR), is displayed on the outside of *E. coli* (grey arrow). Mutants with improved arylsulfatase activity were selected by a 4-step screening procedure (red arrow): **1**) droplet generation and fluorescence assisted droplet sorting (FADS), followed by **2**) agarplate activity screening, **3**) testing of initial reaction rates and **4**) whole cell-based approximation of Michaelis-Menten kinetics. For a more detailed description of all 4 step see Figure 2 and 3.

(*E. coli*, as compared to yeast) that can deal with homo-oligomeric proteins such as *Sp*AS1.[37] Thus far, autodisplay has been used to screen enzyme libraries by binding artificial substrates at the cell surface,[38,39] but has not yet been used for direct detection of enzymatic turnover. We describe a screening procedure for selecting improved variants of the well-characterized arylsulfatase from *Silicibacter pomeroyi* (*Sp*AS1).[37,40] We screened two separate error-prone PCR-generated mutant libraries based on *Sp*AS1^{WT} for improved sulfatase activity using a lysis-free 4-step screening procedure (Figure 1). We identified in total 16 *Sp*AS1 variants with up to 6.2-fold improved sulfatase activity that contain altogether >20 different mutations. Combination of the mutations found in the most active variants selected from the random mutagenesis libraries resulted in an up to 28-fold improvement of the sulfatase activity of *Sp*AS1.

Results and Discussion

Display of active *Sp*AS1 on the surface of *E. coli*

The dimeric arysulfatase *Sp*AS1[37,40] was fused to a gene III secretion signal (N-terminus) and an autotransporter protein (C-terminus) (Figure 2 and Figure S1), as described previously for a wide variety of other proteins.[35,41,42] Successful display of active *Sp*AS1 on the surface of *E. coli* was first shown by testing whole cells expressing the autodisplay construct for activity toward sulfate monoesters **2a** and **3a** (Figure 3). Cells displaying the catalytically inactive *Sp*AS1 C53A variant (k_{cat}/K_M $\sim 10^5$-fold below wild type) or cells containing the empty autodisplay expression vector showed no detectable hydrolysis of sulfate monoesters. SDS-PAGE analysis of the membrane proteins of cells expressing the *Sp*AS1-autotransporter construct showed that the latter is attached to *E. coli* membrane. The same analysis after treatment of cells expressing the *Sp*AS1-autotransporter complex with a protease showed removal of the *Sp*AS1-domain, indicating that *Sp*AS1 is indeed displayed toward the outside of the *E. coli* cells (Figure S2).

Screening of an error-prone-PCR-generated library of displayed *Sp*AS1 variants

We created two different libraries of autodisplayed *Sp*AS1 variants, containing mutations introduced using error-prone PCR with mutagenic nucleotides dPTP and 8-oxo-dGTP respectively (Table S1). Expression of both libraries was induced in *E. coli* in a high cell density bulk solution (Figure 2). The cells displaying the *Sp*AS1 variants were encapsulated in water-in-oil microdroplets containing fluorescein disulfate (sulfate monoester **1a**, Figure 2), according to a Poisson distribution ($\lambda \approx 0.35$). Hydrolysis of fluorescein disulfate into the fluorophore fluorescein (product **1b**, Figure 2) by an active autodisplayed *Sp*AS1 variant allows for fluorescence activated droplet sorting (FADS).[21,25,27] We sorted through $>10^6$ microdroplets until $\sim$4000 microdroplets with at least 2-fold higher fluorescence signal than wild type were collected (Table S1, Figure S5). The sorted positive cells were re-grown into to full-sized colonies on a nitrocellulose filter placed on top of solid growth medium (Figure 2).

The regrown colonies were tested in a second screening step for activity toward sulfate **2a** (Figure 3A). Colonies in which *Sp*AS1-catalyzed conversion of sulfate **2a** resulted in formation of blue chromophore **2b** (Figure 3A, Figure S6) within 30 minutes, were selected for the third screening step. For screening step 3, we tested for improved activity toward 4-nitrophenyl sulfate (sulfate monoester **3a**, Figure 3B, Figure S7). All variants that showed >1.4-fold increased activity toward 4-nitrophenyl sulfate relative to *Sp*AS1^{WT} were selected for the fourth and final step of the screening procedure. In the fourth step we determined the Michaelis-Menten parameters toward 4-nitrophenyl sulfate for the autodisplayed *Sp*AS1 variants (Figure 3C, Figure S10-S11, Table S2-S3). Altogether, 25 *Sp*AS1 variants with improved whole cell second order rates (V_{max}/K_M) were selected and their mutations were determined by DNA sequencing. Out of those 25 selected variants, 7 contained only synonymous mutations, and two variants were found twice (Figure 5A, Figure S12, Table S2-S3). The 16 unique *Sp*AS1 variants that each contain at least 1 non-synonymous mutation were characterized further (see below for details).

The micro-droplet sorting step, during which droplets with a fluorescence signal 2-fold higher than wild-type are selected (Figure S5B and C), is expected to enrich for *E. coli* cells

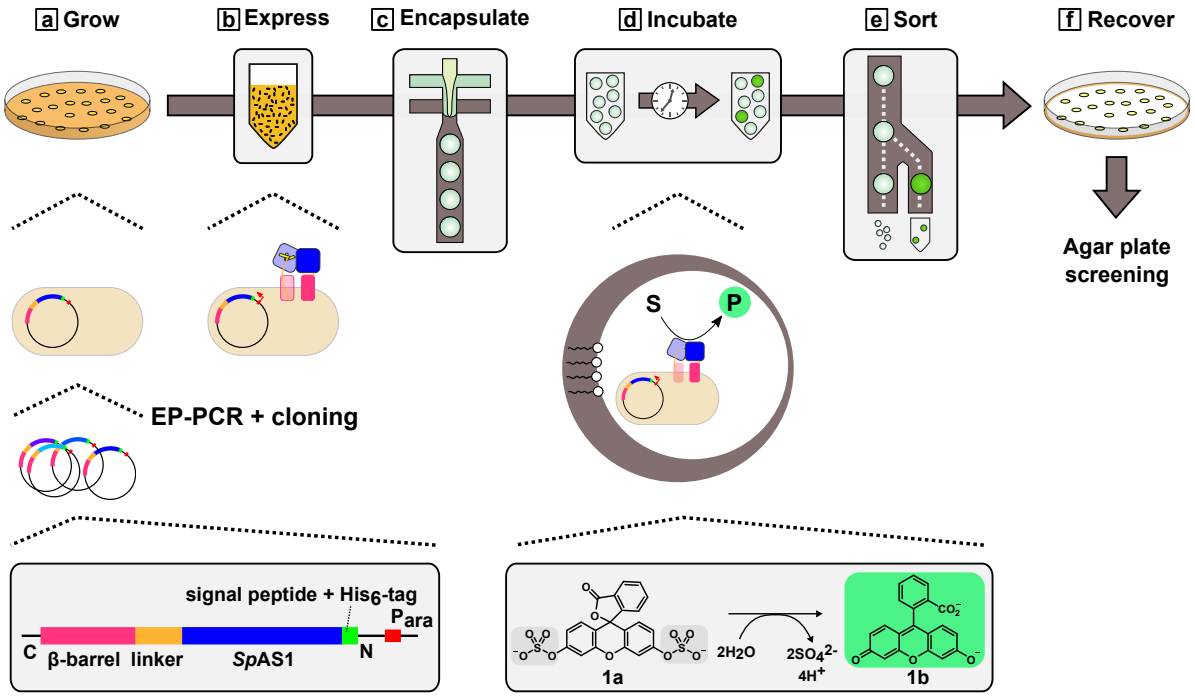

Figure 2: Screening of a library of autodisplayed *Sp*AS1-variants for improved sulfatase activity in microdroplets (step 1 in Figure 1). (**a**) *E. coli* cells containing an error-prone PCR generated mutant library of autodisplayed *Sp*AS1 are grown into full-sized colonies. (**b**) The resulting colonies are resuspended in liquid medium and expression of the the autodisplayed *Sp*AS1 variants is induced in bulk overnight. (**c**) The cells are washed and resuspended in reaction buffer and are encapsulated in water-in-oil microdroplets, each containing 5 µM fluorescein disulfate (sulfate monoester **1a**) and a single *E. coli* cell (the latter in ∼1 in every 3 droplets). (**d**) The droplets are left in the dark at room temperature overnight and (**e**) are subsequently sorted using a custom-built fluorescence activated droplet sorter (FADS). Droplets with a fluorescence signal above the cut-off value are collected directly into a vial containing a mixture of oil, surfactant and recovery medium. (**f**) Once the desired number of sorted events is reached, additional recovery medium containing 0.5% (w/v) pyruvate is added and the cells are allowed to recover for two hours. The recovered cells were plated onto a nitrocellulose filter sitting on top of solid medium and were left to grow into full-sized colonies overnight, ready for screening step 2 (Figure 3A). Details regarding the screening step, library sizes and coverage can be found in the supporting information (Figure S3-S4, Table S1).

displaying highly active *Sp*AS1 variants. In order to assess the effectiveness of the droplet-sorting-based enrichment we also performed the colony-based blue-white screening from step 2 on the 'naive' library, i.e. the library prior to microdroplet-based screening. Comparison between the number of blue variants with activity above the specified threshold (i.e. turn blue after 30 minutes) before and after droplet sorting should inform on the enrichment of screening step 1. Prior to sorting, ∼28% of the colonies in the dPTP-generated library turned blue after 30 minutes, whereas after sorting this percentage rises to ∼42% (∼1.5-fold enrichment). For the 'naive' 8-oxo-dGTP-generated library fewer colonies turn blue before sorting (∼20%) compared to the dPTP library. Furthermore, the 8-oxo-dGTP library shows no apparent enrichment after sorting. Like with the actual screening procedure, we tested the blue colonies from the 'naive' library for activity toward 4-nitrophenyl sulfate.

During the third screening step (Figure 3B) the activities of the *Sp*AS1 variants toward 4-

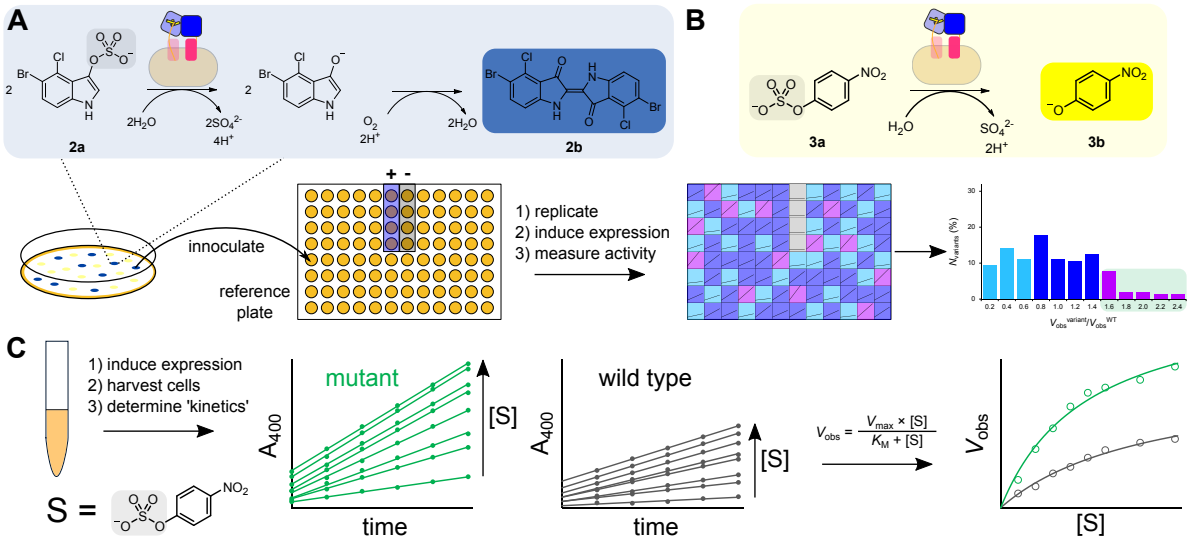

Figure 3: Screening of autodisplayed *Sp*AS1 variants for improved sulfatase activity (steps 2-4 in Figure 1). (**A**) Screening step 2: colonies sitting on top of a nitrocellulose filter expressing active autodisplayed *Sp*AS1 variants are tested for activity toward X-sulfate (**2a**). Colonies displaying active variants that turned blue, due to the formation of chromophore **2b**, within 30 minutes were used to inoculate an individual well in a reference microtiter plate containing growth medium. After overnight growth the reference plate was replicated into another microtiterplate in which expression of the selected *Sp*AS1 variants was induced overnight. (**B**)Screening step 3: activity toward 4-nitrophenyl sulfate (**3a**) was measured as the initial rate of formation of chromophore **3b**, corrected for the measured cell density (OD_{600}). Wild-type and an inactive *Sp*AS1-variant were used for reference and as a negative control respectively. Given the considerable variation in the wild-type control (±30%), only variants with >1.4-fold improved activity were carried over to the final screening step. (**C**) Screening step 4: approximation of Michaelis-Menten parameters of autodisplayed *Sp*AS1 variants for 4-nitrophenyl sulfate (**3a**). Initial rates of 4-nitrophenyl sulfate conversion (V_{obs}) catalyzed by cells displaying *Sp*AS1 variants were determined for 6-8 different substrate concentrations. The resulting data were fitted to Michaelis-Menten kinetics and the resulting parameters V_{max}, K_M and V_{max}/K_M were compared to those of autodisplayed *Sp*AS1^{WT} (see Figure S6-S8 for details).

nitrophenyl sulfate **3a** range from a 10-fold decrease to a >2-fold increase relative to wild-type (Figure 4B and D). We observed a similar range in activities toward 4-nitrophenyl sulfate for the positive variants when droplet sorting is not used as the first screening step, i.e. when screening would start at step 2, omitting step 1 (Figure 4A and C). However, the distributions of the activities toward 4-nitrophenyl sulfate are different when droplet sorting is used as the first step. In fact for both libraries using droplet sorting in the first step results in a 1.6-fold enrichment of significantly improved *Sp*AS1 variants observed during screening step 3 (Figure 4). The use of a different substrate, i.e. sulfate monoester **3a**, may mask the level of enrichment for variants with improved activity toward sulfate monoester **1a**. Furthermore, during droplet sorting, the threshold for scoring a variant as ~2-fold more active than wild-type is based on the assumption that the peak of the activity distribution is at the same postion as the wild-type reference (Figure S5C and D). However, the peak of the activity distribution for sulfate monoester **3a** is at a lower activity than the actual wild-type control in the pre-sort libraries (Figure 4A and C), which could mean that peak of the activity distribution during droplet sorting is also lower than

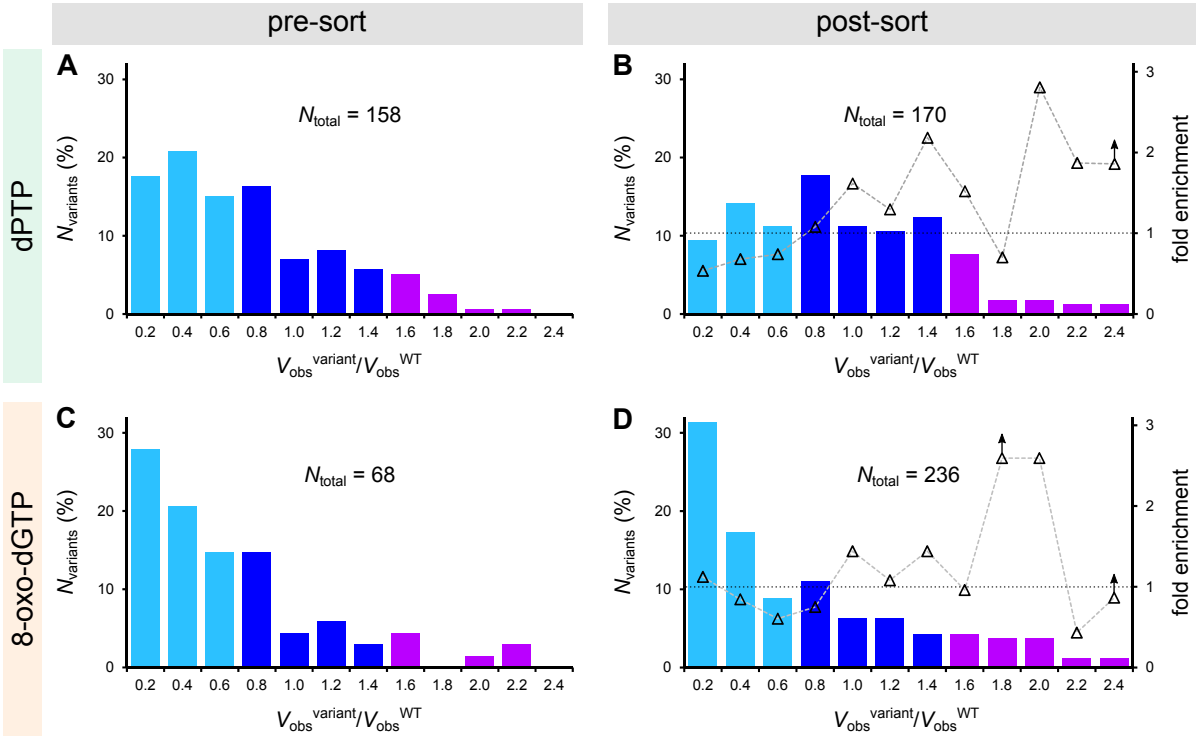

Figure 4: Distribution of active *Sp*AS1-variants before and after fluorescence assisted droplet sorting. *Sp*AS1 variants in each panel were selected after applying screening step 2 (Figure 3A and S6) to the 'naive' libraries (panel **A** and **C**) and after droplet-based activity screening (panel **B** and **D**). The variants are grouped based on the increase/decrease in activity toward 4-nitrophenyl sulfate relative to wild type observed during the screening step described in Figure 3B and S7 ($V_{obs}^{variant}/V_{obs}^{WT}$). Both post-sort histograms show a trend toward increased enrichment with higher $V_{obs}^{variant}/V_{obs}^{WT}$ (triangles). Due to the large variation observed for the wild-type activity ($\pm$30%), all variants for which $V_{obs}^{variant}/V_{obs}^{WT}$ are within 0.6-1.4, are deemed wild-type-like (blue bars). Variants showing >1.4-fold increased activity compared to wild-type (purple bars) in panel B and D were selected for the further screening in step 4.

the actual wild type . Therefore, the 1.5-fold enrichment of improved variants observed in step 3 probably underestimates the actual enrichment achieved during droplet sorting.

Characterization of improved variants

All 16 unique *Sp*AS1 variants that contained at least 1 non-synonymous mutation were subcloned into a vector for cytosolic overexpression (see SI for details), produced in *E. coli* and purified to homogeneity. The improvements in catalytic efficiency (k_{cat}/K_M) toward 4-nitrophenyl sulfate (sulfate monoester **3a**) of these 16 variants range from 1.1- to 6.2-fold (Figure 5B, Table S4). The best variant obtained, *Sp*AS1$^{M111T/K147E}$, showed both a higher rate ($\sim$3-fold increased k_{cat}) and improved apparent binding affinity ($\sim$2-fold decreased K_M). For the other 15 variants, k_{cat} varied relatively little relative to *Sp*AS1^{WT} (0.8-1.5-fold). All 16 variants had increased apparent binding affinity, i.e. a decrease in K_M, with the four best mutants showing the strongest effects (Table S4).

The fusion to the autotransporter could have unexpected effects on the catalytic performance of *Sp*AS1 and as a result the improvements in catalytic efficiencies found during step 4

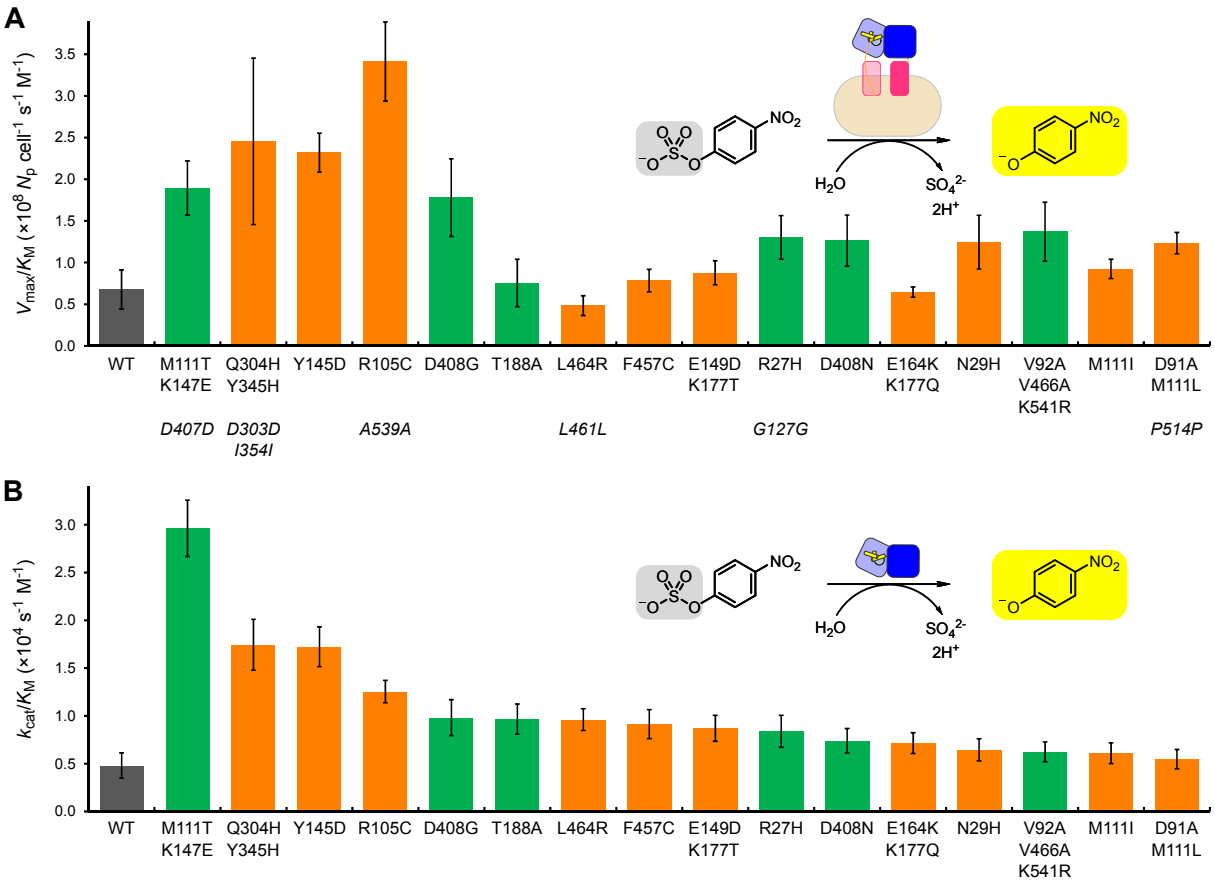

Figure 5: Catalytic performance toward 4-nitrophenyl sulfate of displayed and purified *Sp*AS1-variants selected by the 4-step screening procedure. Mutants indicated in green and orange were generated using dPTP and 8-oxo-dGTP mutagenic nucleotides respectively. (**A**) Michaelis-Menten approximated activity values for autodisplayed *Sp*AS1 variants. (**B**) Catalytic efficiencies for the selected *Sp*AS1 variants. The kinetic parameters for each variant are listed in Tables S2-S4.

for the screening procedure could be different in the purified versions of the respective *Sp*AS1 variants. For example, changes in catalytic rate for the displayed *Sp*AS1 variants (V_{max}) may not correlate with k_{cat} due to variations in the number of *Sp*AS1 molecules displayed (V_{max}=k_{cat}×(N^o of enzyme molecules)). Alternatively, the kinetic parameters (both k_{cat} and K_M) of a particular *Sp*AS1 variant could be affected by the fusion to the autotransporter. These possible differences can have an adverse effect on the reliability of the screening procedure. Since we obtained kinetic parameters for both the autodisplayed (Table S2 and S3) and the purified (Table S4) forms, we are able to determine the correlation between the kinetic parameters of the autodisplayed and purified versions of the selected *Sp*AS1 variants (Figure S15). The apparent binding strength for the autodisplayed ($1/K_M^{\text{whole cells}}$) and purified $K_M^{\text{pure protein}}$ *Sp*AS1 variants show a significant positive correlation ($r = 0.724$; $p = 6.50\times10^{-5}$). Therefore improvements in binding strength ($1/K_M$) in the displayed version of a particular variant is highly likely to translate into improvements in binding strength in the purified version. The reaction rate for whole cells (V_{max}) and the enzymatic rate constant (k_{cat}) show no significant correlation (Figure S15A), most likely due to variations in the number of displayed active *Sp*AS1 molecules per cell as explained above. The correlation between the second order rate con-

stants (V_{max}/K_M *vs.* k_{cat}/K_M) encompasses both parameter correlations (V_{max} *vs.* k_{cat} and $1/K_M^{\text{whole cells}}$ *vs.* $1/K_M^{\text{pure protein}}$) mentioned here. The correlation between these two second order rate constants is positive and significant (r = 0.524; $p = 7.16\times10^{-3}$), suggesting that the positive correlation between $1/K_M^{\text{whole cells}}$ *vs.* $1/K_M^{\text{pure protein}}$ dominates. Furthermore, the correlation for V_{max}/K_M *vs.* k_{cat}/K_M indicates that improvements in V_{max}/K_M for whole cells are a good proxy for improved catalytic efficiency (k_{cat}/K_M) of a given *Sp*AS1 variant.

The 16 improved variants encompass altogether 19 mutated positions. For three residues we find multiple mutations. Residue K177 is located >20 Å away from the active site, on the surface of the protein. Selected mutations at this position occur only in combination with other mutations. The latter could suggest that mutations and this position are enabling the fixation of other mutations, i.e. they are fixed because of epistatic effects. Mutations at position M111 are found both in isolation (M111I) and in combination with other mutations (M111T with K147E; M111L with D91A). Therefore this position could be a hot-spot for both enabling (epistatic) or direct-effect mutations. Mutations in a solvent-exposed aspartate residue located >25Å away form the active site (Figure 6E) result in 2-fold (D408G) and 1.5-fold (D408N) increased catalytic efficiency (Table S4. Another two mutations at the surface, R27H and F457C (Figure 6E), have similar positive effects on the catalytic efficiency (1.8- and 1.9-fold respectively).

The four best *Sp*AS1 variants each contain a mutation in a residue within 8.2 Å of any of the conserved active site residues[37] (mutations R105C, Y145D, K147E and Y345H), whereas for all the other 12 selected variants, mutations only occur in residues >12Å away from the active site. The observation of larger effects on catalytic performance and/or specificity by mutations closer to the active site[43,44] has been observed previously in many directed evolution campaigns involving screening of error-prone PCR-generated libraries.

Interestingly, at a larger scale, i.e. when including 94 closely related dimeric arylsulfatases[37,45] in a multiple sequence alignment, we find that in the 16 improved sequences, only 3 of the 19 positions in which the mutations occur show strong conservation, while all other positions are variable (Figure S16). For the positions analogous to M111 and Q304 in *Sp*AS1, the amino acid found in *Sp*AS1^{WT} is identical to the consensus residue. The consensus amino acid at the position analogous to Y345 is a histidine (Figure S16). Therefore, mutation Y345H is a so-called back-to-consensus mutation.[46] Such mutations are likely to have a stabilizing effect.[47,48] This stabilizing effect has been exploited by enriching the diversity introduced during directed evolution campaigns with back-to-consensus mutations.[47,49–51]

Combination of large effect mutations

To asses if the effects of some observed mutations could be additive, we constructed a mutant in which we combined all six amino acid substitutions of the four most active *Sp*AS1 variants (*Sp*AS1 Σ, Figure 7, Table S5). The combination of two negatively charged residues in close proximity to each other (Y145D and K147E, Figure 6B), can be expected to result in adverse effect on enzyme performance and/or stability. Therefore, we also constructed two variants that avoided this combination, i.e. only Y145D (*Sp*AS1 Σ^{K147}) or K147E (*Sp*AS1 Σ^{Y145}) were present compared to *Sp*AS1 Σ. Indeed, both *Sp*AS1 Σ^{Y145} and *Sp*AS1 Σ^{K147} showed higher catalytic efficiency than *Sp*AS1 Σ (Figure 7, Table S5).

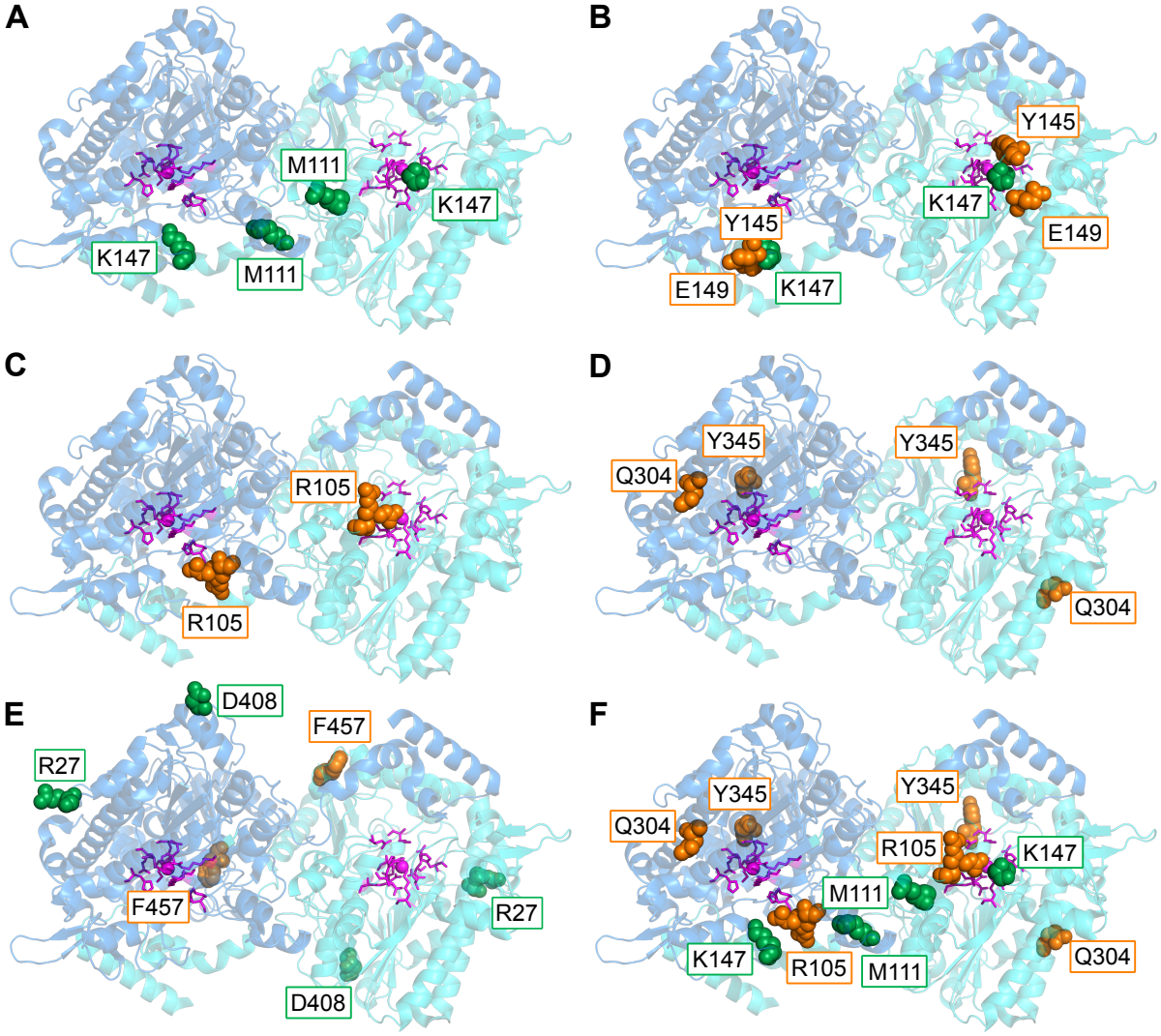

Figure 6: Location of the mutated residues in dimeric *Sp*AS1 (PDB ID for monomer: 4UPI). Mutations indicated in green and orange were introduced during mutagenic PCRs with dPTP and 8-oxo-dGTP nucleotide analogs respectively. The conserved active site residues and the active site metal ion[37,40] are indicated in magenta. (**A**) Positions of the residues that are mutated in the best variant (*Sp*AS1$^{M111T/K147}$). (**B**) Positions of mutated residues in the loop covering the entrance of the active site. (**C**) Position of the mutated residue in *Sp*AS1^{R105C}, a mutant with lowered substrate inhibition (>12-fold increase in K_{SI}) and 2.8-fold improved catalytic efficiency (k_{cat}/K_M). (**D**) Positions of mutated residues in *Sp*AS1$^{Q304H/Y345H}$, a mutant with stronger substrate inhibition (>4-fold decrease in K_{SI}) and 3.5-fold improved catalytic efficiency (k_{cat}/K_M). (**E**) Positions of mutated surface residues that improve sulfatase activity. (**F**) All residues that are mutated in *Sp*AS1 Σ^{Y145} (Figure 7).

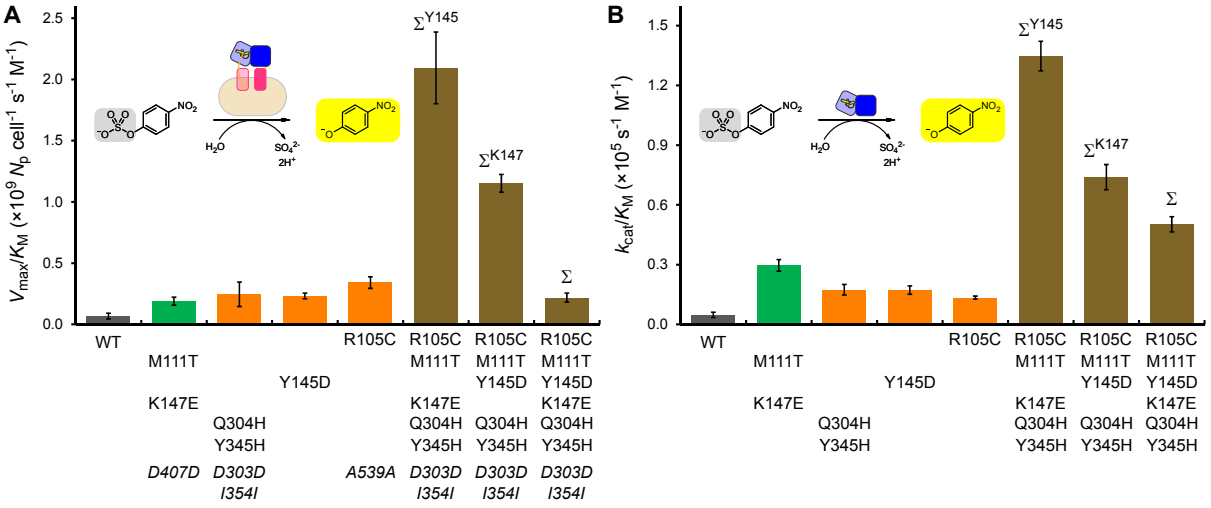

Figure 7: Catalytic performance toward 4-nitrophenyl sulfate of *Sp*AS1-variants containing combinations of the mutations found in the best four mutants. The parent mutants and the wild type are included for comparison. **A**) Michaelis-Menten-approximated activity values (V_{max}/K_M) for autodisplayed *Sp*AS1 variants. **B**) Catalytic efficiencies (k_{cat}/K_M) for the purified *Sp*AS1 variants. The separate kinetic parameters for each variant are listed in Tables S2-S5.

None of the three combination mutants (Σ, Σ^{Y145} and Σ^{K147}) showed improved catalytic rate (k_{cat}) compared to *Sp*AS1$^{M111T/K147E}$. However, all three combination mutants showed an increased apparent binding affinity for sulfate monoester **3a** compared to any of the parent mutants (3.1- to 5.6-fold decrease in K_M). In fact for *Sp*AS1 Σ^{145} the combined effect of the mutations on K_M was close to the expected value if all mutations would be fully additive (11.4-fold (actual) *vs.* 15-fold (expected) decrease in K_M). All three combination mutants showed a higher catalytic efficiency (k_{cat}/K_M) compared to the best variant (*Sp*AS1$^{M111T/K147E}$), although the combined effect was even in the best case not fully additive: the expected maximum effect for Σ^{Y145} is 59-fold, compared to the actual 28-fold improvement we observed. Nevertheless, after a single round of directed evolution toward improved sulfatase activity plus simple combination of the best mutations found after that single round, a 28-fold improvement of an already proficient catalyst ($(k_{cat}/K_M)^{WT}/k_2 = 6.5\times10^{14}$) could be achieved.

Advantages of bacterial autodisplay

Robustness and throughput of the screening procedure are most important for the success of a directed evolution campaign. Throughput determines the likelihood of finding an improved variant and thereby determines the time and effort needed to accomplish a certain degree of improvement. Medium to high throughput detection of sulfatase activity has been accomplished previously, using either conventional agarplate-based and microtiterplate-based methods only[52] or a combination thereof with microdroplets.[21,22,25] For all previous campaigns the sulfatase variants were expressed in the cytosol of *E. coli*. Since negatively charged sulfate esters cannot pass the negatively charged head groups of the phospholipid of the cell membranes, cell lysis was required prior to activity measurements.[21,22,25,52] As a control, we showed that intact *E. coli* cells overexpressing *Sp*AS1 wild-type in their cytosol indeed do not show detectable sulfatase activity.

Displaying a library of enzyme variants on the outside of a cell has several advantages over cell lysis: *i*) it is possible to avoid interfering endogenous activities of cytosolic enzymes present in the host *ii*) in essence only one liquid handling step: mixing of cells and substrate, is required *vs.* at least three steps when using cell lysis (see SI for details) and, *iii*) in particular for microdroplet-based screening, selected genotypes can be directly recovered by cell growth of selected clones, as opposed to the alternative when using cell lysates: recovery of genetic diversity by purification and subsequent re-transformation of plasmid DNA.

The fraction of genetic diversity that can be maximally recovered by plasmid re-transformation is dependent on *i*) the copy number of the plasmid, i.e. how many plasmid molecules can be maximally recovered from the single cell lysate and *ii*) how efficiently the plasmid is re-transformed, i.e. which fraction of the isolated plasmids are successfully transformed and result in the formation of a colony. For small, high copy-number plasmids ($\sim$300 plasmids/cell) that transform efficiently (1 in 18 plasmid molecules is successfully transformed), the genotypic diversity can be recovered multiple times (maximum $\sim$1670%, see SI for details). However, for larger, low copy-number plasmids ($\sim$20 copies/cell) that transform less efficiently (1 in 3661 plasmid molecules is successfully transformed), such as the pBAD-AT-His_6-*Sp*AS1 plasmid we are using here, the maximum recovery of genetic diversity is 0.55% (see SI for details). The live cell re-growth method we used recovered 12% of the sorted diversity, thereby outperforming re-transformation at least >20-fold (see SI for details).

Another advantage, compared e.g. to yeast display, is that our autodisplay system can be used to display libraries of homodimeric enzymes. In yeast display a single protein molecule of interest is linked to either agglutinin or floculation domains which are in turn (covalently) linked to the rigid yeast cell wall.[53] This means that the displayed protein cannot move freely and form homodimers. The autotransporter we fused our libraries of *Sp*AS1-variants to can freely diffuse through the outer membrane of *E. coli*, allowing individual *Sp*AS1 monomers to interact and form homodimers. Furthermore, the use of bacterial autodisplay can be easily implemented to replace any lysis-based screening system for which the widely-used laboratory work horse *E. coli* was previously used, all without drastically changing standard experimental procedures for cell growth and genetic manipulation.

Concluding Remarks

In this study we show, for the first time, the combination of microdroplet-based single variant screening with *E. coli* autodisplay. Using this system we quantitatively screened 10^5-10^6 *Sp*AS1 variants for improved sulfatase activity within several hours. The mobile β-barrel anchor of the autotransporter system facilitated screening a library of random variants of the *homodimeric* sulfatase *Sp*AS1. Such a screen is currently not possible with yeast display, due to the immobility of the 'anchors' that are attached to the displayed protein subunits. Using living *E. coli* cells during the screening steps enabled us to *i*) recover the genotypic diversity after droplet sorting >20-fold more efficient compared to re-transformation-based recovery and *ii*) test for sulfatase activity in microdroplets without cell lysis. Avoiding cell lysis before activity measurements also simplified all subsequent screening steps.

The lysis-free 4-step screening procedure resulted in the identification of 16 mutants with

up to 6.2-fold improved catalytic performance. Mind that previous studies reporting similar or larger improvements after a single round of mutation and screening typically started from enzymes with low efficiencies (k_{cat}/K_M < 30 s^{-1} M^{-1}) toward their desired substrates,[40,52,54,55] while here we improved an already reasonably efficient enzyme (k_{cat}/K_M = 4.8×10^3 s^{-1} M^{-1}) for its *primary* activity. All 19 positions in which mutations were found were non-obvious, i.e. none were previously described conserved active site amino acids.[37,40] The combined effect of five of these non-obvious mutations in *Sp*AS1 Σ^{Y145} shows that a single round of high throughput screening can provide the genetic diversity required to reach an 28-fold improvement in catalytic performance of an already efficient enzyme.

Methods

Construction of plasmid vectors for *E. coli* autodisplay of *Sp*AS1

The previously described dimeric arylsulfatase 1 from *Silicibacter pomeroyi* DSS-3[37,40] (*Sp*AS1) was cloned into autodisplay vector pBAD-AT[42] using standard restriction endonuclease-based cloning using restriction sites *Xho*I and *Kpn*I. Exact experimental details regarding PCR amplification and molecular cloning can be found in the expanded methods.

Initial testing if *Sp*AS1 was displayed as active enzyme was done by testing *E. coli* cells expressing the His_6-*Sp*AS1-autotransporter construct for the ability to catalyze the hydrolysis of 4-nitrophenyl sulfate (sulfate monoester **3a**). As a negative control we used a His_6-*Sp*AS1-autotransporter construct of an inactive *Sp*AS1 variant (C53A, k_{cat}/K_M ∼10^5-fold below wild type). Bacterial culture conditions for expressing the His_6-*Sp*AS1-autotransporter construct are described in detail in the expanded methods. Additional assessment of correct autodisplay of *Sp*AS1 was done essentially as described previously.[56,57] In short, we expressed the His_6-*Sp*AS1-autotransporter construct at 80 mL scale. Half of the cells were treated with proteinase K while the other half was untreated. We subsequently isolated all outer membrane proteins for both treatments and analyzed the protein extracts using SDS-PAGE. Details regarding the bacterial culture conditions, proteinase K treatment and total membrane protein isolation are described in the expanded methods.

Generation of mutant libraries

Genotypic diversity in the *Sp*AS1 libraries was created by two separate error-prone PCR reactions using nucleotide analogs and 2'-deoxy-P-nucleoside-5'-triphosphate (dPTP) and 8-oxo-2'-deoxyguanosine-5'-triphosphate (8-oxo-dGTP) respectively,[58] both in combination with the non-proofreading *Taq* DNA polymerase (Go*Taq*, Promega). The primers used for this PCR reaction anneal outside the His_6-*Sp*AS1 open reading frame (Table S6). The resulting PCR-products were purified and used as a template in an non-mutagenic PCR in order to remove any nucleotide analogs incorporated in the DNA. The non-mutagenic PCR was done essentially as described above, except in this case we used of the same primer pair as with the mutagenic PCR. Cloning of the mutant library into the pBAD-AT vector was essentially done as described above. For each library we sequenced 12 randomly picked library variants to asses the mu-

tation frequencies, which were 2.3±1.7 (dPTP) and 3.7±2.6 (8-oxo-dGTP) non-synonymous base pair substitutions per gene respectively (Table S1).

Library screening procedures

The two different error-prone libraries generated as described above were screened for *Sp*AS1 variants with improved sulfatase activity in four subsequent steps. For all these steps *Sp*AS1 was displayed on the outer membrane of *E. cloni* 10G. During the first step we screened the displayed *Sp*AS1 library for improved activity toward fluorescein disulfate **1a** using a fluorescence activated droplet sorter (FADS, Figure 2 and S3-S4). The cells displaying *Sp*AS1 variants with improved sulfatase activity were regrown to fully sized colonies on a nitrocellulose filter sitting on top of solid medium. For the second step these colonies were tested for improved activity toward 5-bromo-4-chloro-3-indolyl sulfate (X-sulfate **2a**, Figure 3A and S6). All variants that turned visibly blue within 30 minutes after exposure to X-sulfate **2a** were scored as positive. In the third step these positive clones were tested for improved turnover rates of 4-nitrophenyl sulfate **3a** at sub-saturating substrate concentrations (i.e. at $[S] \ll K_M$) (Figure 3B and S7). Displayed *Sp*AS1 variants that showed >1.4-fold improved activity toward 4-nitrophenyl sulfate **3a** (compared to wild type) were chosen for further testing. In the fourth and final step we approximated Michaelis-Menten parameters V_{max}, K_M and V_{max}/K_M for the displayed *Sp*AS1 variants (see Figure 3C and S8 and expanded methods for details). Mutants that showed significant improvement relative to wild-type in a side-by-side comparison (Figure S10-S11), were chosen for further characterization.

Characterization of *Sp*AS1 variants

All 16 unique autodisplayed *Sp*AS1 variants selected after the fourth screening step that contain at least one *non*-synonymous mutation were selected for more detailed characterization. The corresponding *Sp*AS1 variant-encoding genes were cloned into the pASKIBA5$^+$ vector. The resulting N-terminally strep-tagged *Sp*AS1 variants were produced in *E. coli* TOP10 and purified to homogeneity. Determination of kinetic parameters (k_{cat}, K_M, K_{SI} and k_{cat}/K_M) toward 4-nitrophenyl sulfate **3a** for the purified *Sp*AS1-variants was essentially done as described previously.[37,40] The detailed procedures for cloning, protein production and purification, and kinetic measurements are described in the expanded methods.

Construction of the combination mutants

The mutations found in the four best mutants (Figure 5) were combined in a single protein in three different combinations (Figure 7). The combination mutants were created by using several subsequent overlap extension PCR reactions (see expanded methods for details). The resulting PCR product was ligated into the pBAD-AT vector as described above for the wild-type. The pASKIBA5$^+$-constructs of these combination mutants were created in the same way as for all other variants.

Associated content

Supporting information containing further details about the used methods and microfluidic devices, additional discussion, and all kinetic data is available.

Acknowledgements

This research was funded by the Human Frontier Science Program (to F.H. and E.B.B.; grant number RGP0006/2013). P.M. holds a studentship from the Engineering and Physical Sciences Research Council (EP/L015889/1). A.Z. was supported by the BBSRC, the Cambridge Home and EU Scholarship Scheme (CHESS) and the EU Marie-Curie networks PhosChemRec (FP7-PEOPLE ITN-2009-238679) and ENEFP (FP7-PEOPLE-2007-1-1-ITN-215560). J.S. was funded by a fellowship of the Federal Ministry of Education and Research as part of a project within “Bioindustrie 2021” (funding reference: 0316163B). B.D.G.E holds a fellowship from the European Community’s Innovative Training Network ES-cat (722610), F.H. is an ERC Advanced Investigator (695669).

References

(1) Shivange, A. V.; Marienhagen, J.; Mundhada, H.; Schenk, A.; Schwaneberg, U. Advances in Generating Functional Diversity for Directed Protein Evolution. *Curr. Opin. Chem Biol.* **2009**, *13*, 19–25.

(2) Ruff, A. J.; Dennig, A.; Schwaneberg, U. To Get what we Aim for–Progress in Diversity Generation Methods. *FEBS J.* **2013**, *280*, 2961–2978.

(3) Tee, K. L.; Wong, T. S. Polishing the Craft of Genetic Diversity Creation in Directed Evolution. *Biotechnol. Adv.* **2013**, *31*, 1707–1721.

(4) Bratulic, S.; Badran, A. H. Modern Methods for Laboratory Diversification of Biomolecules. *Curr. Opin. Chem. Biol.* **2017**, *41*, 50–60.

(5) Dalby, P. A. Optimising Enzyme Function by Directed Evolution. *Curr. Opin. Struct. Biol.* **2003**, *13*, 500–505.

(6) Packer, M. S.; Liu, D. R. Methods for the Directed Evolution of Proteins. *Nat. Rev. Genet.* **2015**, *16*, 379–394.

(7) Reetz, M. T.; Brunner, B.; Schneider, T.; Schulz, F.; Clouthier, C. M.; Kayser, M. M. Directed Evolution as a Method to Create Enantioselective Cyclohexanone Monooxygenases for Catalysis in Baeyer-Villiger Reactions. *Angew. Chem. Int. Ed.* **2004**, *43*, 4075–4078.

(8) Van Loo, B.; Lutje-Spelberg, J. H.; Kingma, J.; Sonke, T.; Wubbolts, M. G.; Janssen, D. B. Directed Evolution of Epoxide Hydrolase from *A. radiobacter* toward Higher Enantioselectivity by Error-prone PCR and DNA Shuffling. *Chem. Biol.* **2004**, *11*, 981–990.

(9) Kim, J.; Kim, S.; Yoon, S.; Hong, E.; Ryu, Y. Improved Enantioselectivity of Thermostable Esterase from *Archaeoglobus fulgidus* toward (*S*)-Ketoprofen Ethyl Ester by Directed Evolution and Characterization of Mutant Esterases. *Appl. Microbiol. Biotechnol.* **2015**, *99*, 6293–6301.

(10) Wen, S.; Tan, T.; Zhao, H. Improving the Thermostability of Lipase Lip2 from *Yarrowia lipolytica*. *J. Biotechnol.* **2012**, *164*, 248–253.

(11) Poor, C. B.; Andorfer, M. C.; Lewis, J. C. Improving the Stability and Catalyst Lifetime of the Halogenase RebH by Directed Evolution. *ChemBioChem* **2014**, *15*, 1286–1289.

(12) Li, G.; Maria-Solano, M. A.; Romero-Rivera, A.; Osuna, S.; Reetz, M. T. Inducing High Activity of a Thermophilic Enzyme at Ambient Temperatures by Directed Evolution. *Chem. Commun.* **2017**, *53*, 9454–9457.

(13) Wang, Y.; Li, X.; Chen, X.; Chen, D. Directed Evolution and Characterization of Atrazine Chlorohydrolase Variants with Enhanced activity. *Biochemistry (Mosc).* **2013**, *78*, 1104–1111.

(14) Luo, X. J.; Zhao, J.; Li, C. X.; Bai, Y. P.; Reetz, M. T.; Yu, H. L.; Xu, J. H. Combinatorial Evolution of Phosphotriesterase toward a Robust Malathion Degrader by Hierarchical Iteration Mutagenesis. *Biotechnol. Bioeng.* **2016**.

(15) Pikkemaat, M. G.; Janssen, D. B. Generating Segmental Mutations in Haloalkane Dehalogenase: a Novel Part in the Directed Evolution Toolbox. *Nucleic Acids Res.* **2002**, *30*, E35–35.

(16) Gabor, E. M.; Janssen, D. B. Increasing the Synthetic Performance of Penicillin Acylase PAS2 by Structure-inspired Semi-random Mutagenesis. *Protein Eng. Des. Sel.* **2004**, *17*, 571–579.

(17) Liu, J. W.; Boucher, Y.; Stokes, H. W.; Ollis, D. L. Improving Protein Solubility: the Use of the *Escherichia coli* Dihydrofolate Reductase Gene as a Fusion Reporter. *Protein Expr. Purif.* **2006**, *47*, 258–263.

(18) Porter, J. L.; Rusli, R. A.; Ollis, D. L. Directed Evolution of Enzymes for Industrial Biocatalysis. *ChemBioChem* **2016**, *17*, 197–203.

(19) Agresti, J. J.; Antipov, E.; Abate, A. R.; Ahn, K.; Rowat, A. C.; Baret, J. C.; Marquez, M.; Klibanov, A. M.; Griffiths, A. D.; Weitz, D. A. Ultrahigh-throughput Screening in Drop-Based Microfluidics for Directed Evolution. *Proc. Natl. Acad. Sci. U. S. A.* **2010**, *107*, 4004–4009.

(20) Kintses, B.; van Vliet, L. D.; Devenish, S. R.; Hollfelder, F. Microfluidic Droplets: New Integrated Workflows for Biological Experiments. *Curr. Opin. Chem. Biol.* **2010**, *14*, 548–555.

(21) Kintses, B.; Hein, C.; Mohamed, M. F.; Fischlechner, M.; Courtois, F.; Laine, C.; Hollfelder, F. Picoliter Cell Lysate Assays in Microfluidic Droplet Compartments for Directed Enzyme Evolution. *Chem. Biol.* **2012**, *19*, 1001–1009.

(22) Zinchenko, A.; Devenish, S. R.; Kintses, B.; Colin, P. Y.; Fischlechner, M.; Hollfelder, F. One in a Million: Flow Cytometric Sorting of Single Cell-lysate Assays in Monodisperse Picolitre Double Emulsion Droplets for Directed Evolution. *Anal. Chem.* **2014**, *86*, 2526–2533.

(23) Courtois, F.; Olguin, L. F.; Whyte, G.; Bratton, D.; Huck, W. T.; Abell, C.; Hollfelder, F. An Integrated Device for Monitoring Time-dependent *In vitro* Expression from Single Genes in Picolitre Droplets. *ChemBioChem* **2008**, *9*, 439–446.

(24) Mazutis, L.; Baret, J. C.; Treacy, P.; Skhiri, Y.; Araghi, A. F.; Ryckelynck, M.; Taly, V.; Griffiths, A. D. Multi-step Microfluidic Droplet Processing: Kinetic Analysis of an *In vitro* Translated Enzyme. *Lab Chip* **2009**, *9*, 2902–2908.

(25) Colin, P. Y.; Kintses, B.; Gielen, F.; Miton, C. M.; Fischer, G.; Mohamed, M. F.; Hyvonen, M.; Morgavi, D. P.; Janssen, D. B.; Hollfelder, F. Ultrahigh-throughput Discovery of Promiscuous Enzymes by Picodroplet Functional Metagenomics. *Nat. Commun.* **2015**, *6*, 10008.

(26) Mair, P.; Gielen, F.; Hollfelder, F. Exploring Sequence Space in Search of Functional Enzymes Using Microfluidic Droplets. *Curr. Opin. Chem. Biol.* **2017**, *37*, 137–144.

(27) Baret, J. C.; Miller, O. J.; Taly, V.; Ryckelynck, M.; El-Harrak, A.; Frenz, L.; Rick, C.; Samuels, M. L.; Hutchison, J. B.; Agresti, J. J.; Link, D. R.; Weitz, D. A.; Griffiths, A. D. Fluorescence-activated Droplet Sorting (FADS): Efficient Microfluidic Cell Sorting Based on Enzymatic Activity. *Lab Chip* **2009**, *9*, 1850–1858.

(28) Gielen, F.; Hours, R.; Emond, S.; Fischlechner, M.; Schell, U.; Hollfelder, F. Ultrahigh-throughput-Directed Enzyme Evolution by Absorbance-Activated Droplet Sorting (AADS). *Proc. Natl. Acad. Sci. U. S. A.* **2016**, *113*, E7383–E7389.

(29) Gielen, F.; Butz, M.; Rees, E. J.; Erdelyi, M.; Moschetti, T.; Hyvonen, M.; Edel, J. B.; Kaminski, C. F.; Hollfelder, F. Quantitative Affinity Determination by Fluorescence Anisotropy Measurements of Individual Nanoliter Droplets. *Anal. Chem.* **2017**, *89*, 1092–1101.

(30) Leemhuis, H.; Stein, V.; Griffiths, A. D.; Hollfelder, F. New genotype-phenotype linkages for directed evolution of functional proteins. *Curr. Opin. Struct. Biol.* **2005**, *15*, 472–478.

(31) Soumillion, P.; Fastrez, J. Novel Concepts for Selection of Catalytic Activity. *Curr. Opin. Biotechnol.* **2001**, *12*, 387–394.

(32) Amstutz, P.; Pelletier, J. N.; Guggisberg, A.; Jermutus, L.; Cesaro-Tadic, S.; Zahnd, C.; Pluckthun, A. *In vitro* Selection for Catalytic Activity with Ribosome Display. *J. Am. Chem. Soc.* **2002**, *124*, 9396–9403.

(33) Betley, J. R.; Cesaro-Tadic, S.; Mekhalfia, A.; Rickard, J. H.; Denham, H.; Partridge, L. J.; Pluckthun, A.; Blackburn, G. M. Direct Screening for Phosphatase Activity by Turnover-based Capture of Protein Catalysts. *Angew. Chem. Int. Ed. Engl.* **2002**, *41*, 775–777.

(34) Cesaro-Tadic, S.; Lagos, D.; Honegger, A.; Rickard, J. H.; Partridge, L. J.; Blackburn, G. M.; Pluckthun, A. Turnover-based *In vitro* Selection and Evolution of Biocatalysts from a Fully Synthetic Antibody Library. *Nat. Biotechnol.* **2003**, *21*, 679–685.

(35) Jose, J.; Maas, R. M.; Teese, M. G. Autodisplay of Enzymes–Molecular Basis and Perspectives. *J. Biotechnol.* **2012**, *161*, 92–103.

(36) Quehl, P.; Hollender, J.; Schuurmann, J.; Brossette, T.; Maas, R.; Jose, J. Co-expression of active human cytochrome P450 1A2 and cytochrome P450 reductase on the cell surface of *Escherichia coli*. *Microb. Cell Fact.* **2016**, *15*, 26.

(37) Van Loo, B.; Bayer, C. D.; Fischer, G.; Jonas, S.; Valkov, E.; Mohamed, M. F.; Vorobieva, A.; Dutruel, C.; Hyvonen, M.; Hollfelder, F. Balancing Specificity and Promiscuity in Enzyme Evolution: Multidimensional Activity Transitions in the Alkaline Phosphatase Superfamily. *J. Am. Chem. Soc. In revision* **2018**, *xx*, yy–yy.

(38) Becker, S.; Michalczyk, A.; Wilhelm, S.; Jaeger, K. E.; Kolmar, H. Ultrahigh-throughput Screening to Identify *E. coli* Cells Expressing Functionally Active Enzymes on their Surface. *ChemBioChem* **2007**, *8*, 943–949.

(39) Becker, S.; Hoebenreich, H.; Vogel, A.; Knorr, J.; Wilhelm, S.; Rosenau, F.; Jaeger, K. E.; Reetz, M. T.; Kolmar, H. Single-cell High-throughput Screening to Identify Enantioselective Hydrolytic Enzymes. *Angew. Chem. Int. Ed.* **2008**, *47*, 5085–5088.

(40) Bayer, C. D.; van Loo, B.; Hollfelder, F. Specificity Effects of Amino Acid Substitutions in Promiscuous Hydrolases: Context-Dependence of Catalytic Residue Contributions to Local Fitness Landscapes in Nearby Sequence Space. *ChemBioChem* **2017**, *18*, 1001–1015.

(41) Schüürmann, J.; Quehl, P.; Festel, G.; Jose, J. Bacterial Whole-cell Biocatalysts by Surface Display of Enzymes: toward Industrial Application. *Appl. Microbiol. Biotechnol.* **2014**, *98*, 8034–8046.

(42) Strohle, F. W.; Kranen, E.; Schrader, J.; Maas, R.; Holtmann, D. A Simplified Process Design for P450 Driven Hydroxylation Based on Surface Displayed Enzymes. *Biotechnol. Bioeng.* **2016**, *113*, 1225–1233.

(43) Morley, K. L.; Kazlauskas, R. J. Improving Enzyme Properties: When Are Closer Mutations Better? *Trends Biotechnol.* **2005**, *23*, 231–237.

(44) Rahimi, M.; van der Meer, J. Y.; Geertsema, E. M.; Poddar, H.; Baas, B. J.; Poelarends, G. J. Mutations Closer to the Active Site Improve the Promiscuous Aldolase Activity of 4-Oxalocrotonate Tautomerase More Effectively than Distant Mutations. *ChemBioChem* **2016**, *17*, 1225–1228.

(45) Van Loo, B.; Schober, M.; Valkov, E.; Heberlein, M.; Bornberg-Bauer, E.; Faber, K.; Hyvonen, M.; Hollfelder, F. Structural and Mechanistic Analysis of the Choline Sulfatase from *Sinorhizobium melliloti*: A Class I Sulfatase Specific for an Alkyl Sulfate Ester. *J. Mol. Biol.* **2018**, *430*, 1004–1023.

(46) Bershtein, S.; Goldin, K.; Tawfik, D. S. Intense Neutral Drifts Yield Robust and Evolvable Consensus Proteins. *J. Mol. Biol.* **2008**, *379*, 1029–1044.

(47) Jones, B. J.; Lim, H. Y.; Huang, J.; Kazlauskas, R. J. Comparison of Five Protein Engineering Strategies for Stabilizing an α/β-Hydrolase. *Biochemistry* **2017**, *56*, 6521–6532.

(48) Gomez-Fernandez, B. J.; Garcia-Ruiz, E.; Martin-Diaz, J.; Gomez de Santos, P.; Santos-Moriano, P.; Plou, F. J.; Ballesteros, A.; Garcia, M.; Rodriguez, M.; Risso, V. A.; Sanchez-Ruiz, J. M.; Whitney, S. M.; Alcalde, M. Directed -*In Vitro*- Evolution of Precambrian and Extant Rubiscos. *Sci Rep* **2018**, *8*, 5532.

(49) Aerts, D.; Verhaeghe, T.; Joosten, H. J.; Vriend, G.; Soetaert, W.; Desmet, T. Consensus Engineering of Sucrose Phosphorylase: the Outcome Reflects the Sequence Input. *Biotechnol. Bioeng.* **2013**, *110*, 2563–2572.

(50) Nakano, S.; Asano, Y. Protein Evolution Analysis of *S*-Hydroxynitrile Lyase by Complete Sequence Design Utilizing the INTMSAlign Software. *Sci. Rep.* **2015**, *5*, 8193.

(51) Porebski, B. T.; Buckle, A. M. Consensus Protein Design. *Protein Eng. Des. Sel.* **2016**, *29*, 245–251.

(52) Miton, C. M.; Jonas, S.; Fischer, G.; Duarte, F.; Mohamed, M. F.; van Loo, B.; Kintses, B.; Kamerlin, S. C. L.; Tokuriki, N.; Hyvonen, M.; Hollfelder, F. Evolutionary Repurposing of a Sulfatase: A New Michaelis Complex Leads to Efficient Transition State Charge Offset. *Proc. Natl. Acad. Sci. U. S. A.* **2018**, *115*, E7293–E7302.

(53) Kondo, A.; Ueda, M. Yeast Cell-surface Display–Applications of Molecular Display. *Appl. Microbiol. Biotechnol.* **2004**, *64*, 28–40.

(54) Meier, M. M.; Rajendran, C.; Malisi, C.; Fox, N. G.; Xu, C.; Schlee, S.; Barondeau, D. P.; Hocker, B.; Sterner, R.; Raushel, F. M. Molecular Engineering of Organophosphate Hydrolysis Activity from a Weak Promiscuous Lactonase Template. *J. Am. Chem. Soc.* **2013**, *135*, 11670–11677.

(55) Uduwela, D. R.; Pabis, A.; Stevenson, B. J.; Kamerlin, S. C. L.; McLeod, M. D. Enhancing the Steroid Sulfatase Activity of the Arylsulfatase from *Pseudomonas aeruginosa*. *ACS. Catal.* **2018**, *8*, 8902–8914.

(56) Park, M.; Yoo, G.; Bong, J.; Jose, J.; Kang, M.; Pyun, J. Isolation and Characterization of the Outer Membrane of *Escherichia coli* with Autodisplayed Z-domains. *Biochim. Biophys. Acta* **2015**, *1848*, 842–847.

(57) Yoo, G.; Dilkaute, C.; Bong, J.; Song, H.; Lee, M.; Kang, M.; Jose, J.; Pyun, J. Autodisplay of the La/SSB Protein on LPS-free *E. coli* for the Diagnosis of Sjögren's Syndrome. *Enz. Microb. Technol.* **2017**, *100*, 1–10.

(58) Zaccolo, M.; Williams, D. M.; Brown, D. M.; Gherardi, E. An Approach to Random Mutagenesis of DNA Using Mixtures of Triphosphate Derivatives of Nucleoside Analogues. *J. Mol. Biol.* **1996**, *255*, 589–603.

Table of contents graphic